Phosphorylation of XIAP by CDK1-cyclin B controls mitotic cell death

Hou, Yingping; Allan, Lindsey A.; Clarke, Paul R.

Published in:
Journal of Cell Science

DOI:
10.1242/jcs.192310

Publication date:
2017

Document Version
Publisher's PDF, also known as Version of record

Phosphorylation of XIAP by CDK1-cyclin B controls mitotic cell death

Ying Hou, Lindsey A. Allan and Paul R. Clarke*

Division of Cancer Research

School of Medicine

University of Dundee

Jacqui Wood Cancer Centre

Ninewells Hospital and Medical School

Dundee DD1 9SY

Scotland, U.K.

* Author for correspondence

p.r.clarke@dundee.ac.uk

Tel. +44 (0)1382 383247

Fax. +44 (0)1382 386419

Key words: Mitosis, apoptosis, cell death, caspase.

Journal of Cell Science • Advance article

JCS Advance Online Article. Posted on 7 December 2016

SUMMARY STATEMENT

This work identifies a molecular mechanism that controls the onset of mitotic cell death, which is important for surveillance against defects in mitosis and the response to cancer drugs that target cell division.

ABSTRACT

Regulation of cell death is critical for the response of cancer cells to drug treatments that cause arrest in mitosis, and is likely to be important for protection against chromosome instability in normal cells. Prolonged mitotic arrest can result in cell death by activation of caspases and the induction of apoptosis. Here, we show that X-linked inhibitor of apoptosis (XIAP) plays a key role in the control of mitotic cell death. Ablation of XIAP expression sensitises cells to prolonged mitotic arrest caused by a microtubule poison. XIAP is stable during mitotic arrest, but its function is controlled through phosphorylation by the mitotic kinase CDK1-cyclin B1 at Ser40. Mutation of Ser40 to a phospho-mimetic residue (S40D) inhibits binding to activated effector caspases and abolishes the anti-apoptotic function of XIAP, whereas a non-phosphorylated mutant (S40A) blocks apoptosis. By live-cell imaging, we show that phosphorylation of XIAP reduces the threshold for the onset of cell death in mitosis. This work illustrates that mitotic cell death is a form of apoptosis linked to the progression of mitosis through control by CDK1-cyclin B.

Journal of Cell Science • Advance article

INTRODUCTION

Anti-cancer drugs such as microtubule poisons arrest or delay cells in mitosis due to the action of the mitotic or spindle assembly checkpoint. This checkpoint normally prevents anaphase from occurring before all chromosomes are correctly bi-orientated on the metaphase spindle by inhibition of the anaphase-promoting complex or cyclosome (APC/C), a large E3 ubiquitin ligase complex that targets mitotic regulators such as securin and cyclin B1 for destruction by the proteasome (Primorac and Musacchio, 2013). Cells that are arrested for a prolonged period in mitosis can undergo cell death by the process of apoptosis (Allan and Clarke, 2007; Gascoigne and Taylor, 2008). The propensity for apoptosis is increased by the duration of the mitotic arrest (Bekier et al., 2009; Huang et al., 2009) whereas exit from mitosis generally reduces sensitivity to anti-mitotic drugs (Brito and Rieder, 2006; Gascoigne and Taylor, 2008). Apoptosis can still occur after release from a prolonged delay in mitosis after longer-term changes including activation of signalling pathways and new protein expression (Colin et al., 2015; Uetake and Sluder, 2010).

The intrinsic apoptotic pathway is activated when cytochrome c is released from mitochondria into the cytosol, where it forms a complex with Apaf-1 leading to the recruitment and activation of caspase-9, a cystyl-aspartame endoprotease. Caspase-9 in turn cleaves and activates the effector caspases -3 and -7, which act on multiple substrates to bring about the cellular changes associated with apoptosis, including cellular blebbing, chromatin condensation and internucleosomal DNA fragmentation (Budihardjo et al., 1999). This pathway is controlled during mitosis by protein phosphorylation and the ubiquitin/proteasome-mediated destruction of regulators of the intrinsic apoptotic pathway; these mechanisms couple the control of apoptosis to the progression of mitosis (Clarke and Allan, 2009). Caspase-9 is phosphorylated at an inhibitory site in mitosis by CDK1-cyclin B1, the major mitotic protein kinase, which thereby restrains apoptosis during normal mitosis and the initial stages of mitotic arrest. If metaphase is not successfully resolved then apoptosis is initiated during a prolonged mitotic arrest when the apoptotic signal overcomes the threshold set by caspase-9 phosphorylation (Allan and Clarke, 2007). Conversely, the apoptotic signal is initiated when phosphorylation of the anti-apoptotic protein Mcl-1 at Thr92 by CDK1-cyclin B1 causes it to be degraded during a delay in mitosis (Harley et al., 2010; Wertz et al., 2011). Stabilisation of Mcl-1 by abolition of Thr92 phosphorylation or mutation of a destruction box (D-Box) that is recognised by the APC/C inhibits apoptosis induced by microtubule poisons (Harley et al., 2010). In addition, the related anti-apoptotic proteins Bcl-2 and Bcl-x_L are phosphorylated and appear to be partially inhibited during

mitosis (Terrano et al., 2010). The slow degradation of cyclin B1 even though the spindle assembly checkpoint is active can lead eventually to inactivation of CDK1-cyclin B1 and slippage out of mitosis (Brito and Rieder, 2006). Whether or not apoptosis is initiated during mitotic arrest is likely to depend upon relative changes in the activities of CDK1-cyclin B1 and regulators of apoptosis during the mitotic arrest (Allan and Clarke, 2007; Gascoigne and Taylor, 2008).

Although caspase-3 and caspase-7 do not appear to be regulated directly during mitosis by phosphorylation, these enzymes might also be controlled through interacting proteins. One candidate is XIAP (X-linked inhibitor of apoptosis), a protein of the IAP family that is capable of inhibiting activated caspases-3, -7 and -9 by direct binding (Deveraux et al., 1999; Takahashi et al., 1998). XIAP can also function as an E3 ubiquitin ligase and as a signal transduction intermediate (Eckelman et al., 2006; Lu et al., 2007). XIAP is over-expressed in a number of cancer cell lines and its over-expression correlates with increased resistance to chemotherapeutic drugs, including inhibitors of mitosis (Durie et al., 2011; Holcik et al., 2000; Tamm et al., 2000).

XIAP is regulated acutely by post-translational modifications that can determine sensitivity to cellular stresses: phosphorylation at serine 87 by Akt reduces XIAP auto-ubiquitylation and stabilises the protein in cisplatin-treated cells (Dan et al., 2004) whereas phosphorylation at serine 430 by TANK-binding kinase 1 (TBK1) or IκB kinase IKKε results in the auto-ubiquitylation and subsequent proteasomal degradation of XIAP after viral infection of cells (Nakhaei et al., 2012). However, it has been unclear if regulation of XIAP plays a role in controlling apoptosis during mitosis. In this study, we show that XIAP is phosphorylated at specific sites during mitosis by CDK1-cyclin B, which inhibits the anti-apoptotic activity of XIAP and makes mitotic cells more sensitive to pro-apoptotic signals. Thus, XIAP plays a key role in coupling the control of apoptosis to the progression of mitosis.

RESULTS

XIAP restrains apoptosis in response to prolonged mitotic arrest

We tested the role of human XIAP in the control of apoptosis in response to the disruption of mitosis. We found that ablation of XIAP in U2OS cells by siRNA promoted the cleavage and activation of caspase-3, a major effector of apoptosis (Figure 1A,B; Supplementary figure 1A), and caused sub-G1 apoptotic fragmentation of DNA (Figure 1C; Supplementary figure 1B) after prolonged treatment of the cells with nocodazole, a microtubule poison that prevents mitotic spindle assembly and arrests cells in mitosis. Entirely consistent with these results, there was increased active caspase-3 and sub-G1 DNA fragmentation in XIAP-/- HCT116 cells compared to wild-type cells after prolonged treatment with nocodazole (Supplementary figure 1C,D). Thus, XIAP plays a role in the restraint of apoptosis in response to prolonged mitotic arrest.

XIAP is phosphorylated during mitosis

Although these results established that XIAP plays a role in the control of apoptosis in response to prolonged mitotic arrest, we did not observe any periodic changes in the levels of the protein during the cell cycle (Supplementary figure 2A), which might indicate a mechanism of regulation. Similarly, the level of XIAP was maintained during a prolonged mitotic arrest until exit from mitosis and the induction of apoptosis (Supplementary figure 2B). To determine if XIAP is regulated post-translationally by phosphorylation during mitosis, we treated HeLa and U2OS cells with nocodazole and compared isolated rounded-up mitotic cells with adherent interphase cells. Modification of XIAP leading to retardation of the protein was not readily detected on Western blots of conventional SDS-PAGE gels (Figure 2A). However, modification of XIAP in mitotic cells was clearly apparent when gels were supplemented with PhosTag, an acrylamide-bound ligand that preferentially retards the migration of phosphorylated proteins (Kinoshita et al., 2006). There was one major and one minor retarded form of XIAP in rounded-up mitotic cells, but not in adherent interphase cells also treated with nocodazole nor in untreated asynchronous cells, demonstrating that XIAP was phosphorylated on at least two sites specifically during mitosis, with one site predominating (Figure 2A). XIAP was also phosphorylated in mitotic HCT116 and DLD1 human colorectal cancer cells with a very similar pattern of phosphorylated forms (Figure 2B).

The mitotic phosphorylation of XIAP was reversed in parallel with cyclin B degradation when U2OS cells were released from mitotic arrest by washing out nocodazole. Dephosphorylation of XIAP was prevented by the proteasome inhibitor MG132, which prevents the degradation of cyclin B even in the absence of the checkpoint signal and maintains cells in mitosis (Figure 2C). When mitotically-arrested cells were maintained in nocodazole having been synchronised in the period of the arrest, phosphorylated forms of XIAP progressively accumulated over 2-6 hours. MG132 did not alter the pattern of phosphorylated forms during mitotic arrest, indicating that both hypo- and hyper-phosphorylated XIAP were stable during the period of arrest (Figure 2D).

Purified recombinant XIAP expressed as a fusion protein with glutathione-S-transferase (GST-XIAP) was also phosphorylated in a mitotic HeLa cell extract, with one major retarded form observed on PhosTag gels that accumulated over 30 mins (Figure 2E). Formation of phosphorylated XIAP form was inhibited by calf intestinal phosphatase (CIP) or inhibition of cyclin-dependent kinases (CDKs) by purvalanol A (PA) (Figure 2F), indicating mitotic phosphorylation of this major site is dependent on CDK1 in complex with cyclin B rather than cyclin A, which is lost from mitotically-arrested cells prior to preparation of the extract.

Identification of sites of mitotic phosphorylation in XIAP

Human XIAP contains four serine/threonine residues (Ser40, Ser87, Thr180 and Thr359) that are followed immediately by a proline residue, a characteristic of phosphorylation sites targeted by proline-directed kinases such as CDK1-cyclin B. Ser40 has been identified in a global analysis of phosphorylation sites (Mertins et al., 2013) and Ser87 has been shown to be phosphorylated by Akt (Dan et al., 2004). To analyse these potential mitotic phosphorylation sites, we mutated each residue to a non-phosphorylatable alanine residue and produced the resulting proteins by in vitro transcription and translation (IVT) in mammalian reticulocyte lysate. When incubated in mitotic HeLa cell extract, the wild-type, S87A, T180A and T359A proteins were all phosphorylated whereas mutation of Ser40 abolished the formation of the predominant phosphorylated form (Figure 3A), indicating that this residue was the major phosphorylation site.

In another approach to determine the site(s) of mitotic phosphorylation, XIAP stably expressed as a fusion with green fluorescent protein (GFP-XIAP) was immunoprecipitated from mitotic nocodazole-treated U2OS cells. We confirmed that the protein was indeed phosphorylated in mitosis, exhibiting one major and one minor phosphorylated form (Figure

3B), before analysis of tryptic peptides by nano LC-MS/MS on a LTQ-Obitrap Velos mass spectrometer in combination with a neutral loss scan on a 4000 QTRAP mass spectrometer to detect phosphorylated peptides. Two phosphorylation sites were identified, with a major peptide phosphorylated on Ser40 and a less abundant peptide phosphorylated on Thr180 (Figure 3C). Taking into account the proportion of modified XIAP detected on PhosTag gels, this data shows that approximately 50% of XIAP is phosphorylated at Ser40 in cells arrested in mitosis, with additional phosphorylation at T180 at a lower stoichiometry.

XIAP is phosphorylated at serine 40 in mitosis

To facilitate analysis of the phosphorylation of Ser40 in XIAP, a specific polyclonal antibody was raised by inoculation with a synthetic peptide that included the phosphorylated site. Antibodies were purified from serum by negative selection against the dephosphorylated peptide followed by positive selection against the phosphopeptide. Selectivity was tested on dot blots where BSA-conjugated peptides were probed using purified antibodies (Figure 4A). The pS40 antibody detected IVT XIAP phosphorylated in mitotic HeLa cell extracts, whereas the S40A mutant was not detected. Thus, the antibody is specific for phosphorylated Ser40 and no other phosphorylation site in XIAP (Figure 4B). Endogenous XIAP phosphorylated on Ser40 was detected in U2OS cells arrested in mitosis with nocodazole; the specific polypeptide was identified by its ablation by prior depletion of XIAP by siRNA transfection (Figure 4C).

We confirmed that Ser40 was phosphorylated in GFP-XIAP expressed in U2OS cells arrested in mitosis with nocodazole. Analysis of the migration of GFP-XIAP on PhosTag gels (Figure 4D) showed that mutation of Ser40 inhibited the formation of not only the major phosphorylated form but also other minor phosphorylated forms. This indicates that Ser40 is necessary for phosphorylation at one or more less abundant sites, most likely including Thr180. GFP-XIAP was phosphorylated on Ser40 in mitotic U2OS cells but not in untreated adherent interphase cells or nocodazole-treated adherent cells (Figure 4E). We unequivocally identified this phosphorylated form as GFP-XIAP by its immunoprecipitation from cell extracts prior to Western blotting (Figure 4F).

XIAP is phosphorylated at serine 40 by CDK1-cyclin B

The previous observation that purvalanol A inhibited the phosphorylation of GST-XIAP in mitotic HeLa cell extract (Figure 2F) indicated that phosphorylation was dependent on a CDK1-cyclin B. Similarly, phosphorylation of IVT XIAP incubated in mitotic HeLa cell extract and analysed on a PhosTag gel (Figure 5A) was inhibited by purvalanol A and RO3306, a more selective inhibitor that specifically targets CDK1 and not DYRK1A at the concentration used (Vassilev et al., 2006). We confirmed that CDK inhibitors, but not other kinase inhibitors including wortmannin, inhibited the phosphorylation of Ser40 in XIAP in mitotic extracts (Figure 5B). Futhermore, XIAP was phosphorylated on Ser40 in a time-dependent manner by incubation with purified CDK1-cyclin B1 (Figure 5C), showing that this kinase catalyses the phosphorylation of XIAP directly.

Mutation of serine 40 to aspartate inhibits XIAP binding to active effector caspases.

XIAP is perhaps best known for its ability to bind to and inhibit activate caspases (Deveraux et al., 1999; Takahashi et al., 1998). To test whether mitotic phosphorylation of XIAP at Ser40 could affect this function we carried out an in vitro binding assay utilising a potentially phosphomimetic aspartate mutant (S40D) as a surrogate for phosphorylated XIAP and comparing its ability to bind cleaved effector caspases with that of the non-phosphorylatable mutant S40A. GFP-XIAP S40D and S40A proteins produced in stably transfected U2OS cells were incubated with HeLa cell extract (S100) pretreated with cytochrome *c* and dATP to generate cleaved caspases (Li et al., 1997). Western blotting analysis of proteins co-precipitating from the extract demonstrated that XIAP S40D was less efficient at binding to cleaved caspase 7 and cleaved caspase 3 than the S40A protein (Figure 6). In contrast, both XIAP proteins exhibited a similar ability to bind to Smac, a protein that binds to and neutralises XIAP function (Du et al., 2000; Verhagen et al., 2000). This shows that the S40D protein is competent for some aspects of XIAP function but is inhibited in its ability to bind activated effector caspases, indicating that mitotic phosphorylation of XIAP at Ser40 restrains its ability to inhibit caspase activity.

Modification of XIAP at serine 40 inhibits its anti-apoptotic activity

The inhibitory effect of the S40D mutation on the ability of XIAP to bind active caspases strongly suggests that phosphorylation of Ser40 in XIAP regulates its anti-apoptotic activity. To test this possibility, we first characterised the stability of wild type and phosphorylation site mutant GFP-XIAP proteins during interphase and mitotic arrest. We found that GFP-

XIAP S40A and S40D proteins, like the wild-type protein, were expressed at a constant level during mitotic arrest, indicating that the stability of the protein during mitosis was not affected by phosphorylation at this site (Figure 7A). Consistent with results discussed above (Figure 2D), phosphorylation of Ser40 detected by the specific antibody gradually increased over 2-6h of arrest (Supplementary figure 3). Importantly, while expression of either wild-type XIAP or the S40A mutant strongly inhibited the induction of apoptosis after prolonged treatment with nocodazole, the S40D mutant was much less effective and produced no apparent inhibition of apoptosis (Figure 7B, Supplementary figure 4A). The difference between the S40A and S40D proteins strongly suggests that phosphorylation of Ser40 inhibits the anti-apoptotic activity of XIAP. The similar effect of wild-type and S40A XIAP expression is consistent with the dominant inhibitory activity of the non-phosphorylated protein which is strongly elevated in both cases.

To determine if modification of XIAP at Ser40 affects the acute apoptotic response during mitosis when phosphorylation occurs, we analysed the induction of cell death in individual mitotic cells by live-cell imaging. U2OS cells arrested in mitosis by 250 ng/ml nocodazole were tracked for around 70 h after entry into mitosis, by which time they had either slipped from mitosis, blebbing transiently and flattening down as they entered interphase (denoted survival), or had undergone rigorous blebbing followed by stasis (mitotic cell death) (Figure 7C, Supplementary figure 4B). About 55% of control cells transfected with an empty vector (EV) underwent mitotic cell death and cells that expressed S40D mutant of XIAP showed only a slight reduction in cell death to 40% of control. By contrast, cells expressing either wild-type of S40A mutant of XIAP showed a strong reduction in mitotic cell death (<5% of control) (Figure 7D), indicating that phosphorylation of XIAP at Ser40 inhibits its activity during mitosis and promotes mitotic cell death.

DISCUSSION

The induction of apoptosis during mitosis provides a mechanism to selectively kill rogue cells that have failed to undergo chromosome segregation successfully and on schedule. This pathway also provides opportunities for the selective killing of cancer cells through drugs that interfere with mitosis, including microtubule poisons such as taxanes that prevent the proper attachment of chromosomes to spindle microtubules and cause a prolonged arrest in mitosis due to the activity of the spindle assembly (mitotic) checkpoint. Importantly, there are distinct post-translational mechanisms that control apoptosis during mitosis that facilitate

drug-induced cell killing, perhaps especially in cancer cells that have sustained cellular stress but in which apoptosis is actively suppressed.

In this report we have identified a mechanism that controls the induction of cell death in mitotically-arrested cells through a key regulator, XIAP. Our results indicate that phosphorylation of XIAP at a single major site by the master mitotic kinase, CDK1-cyclin B, negates the ability of XIAP to bind to active effector caspases and thereby reduces the threshold for apoptosis (Figure 8). We show that approximately 50% of the endogenous XIAP protein is phosphorylated at the inhibitory site, Ser40 (Figure 3), suggesting that the remaining protein that is not phosphorylated at this site continues to provide a restraint, albeit reduced, so that when XIAP is completely ablated, apoptosis is increased further (Figure 1). We propose that this mechanism is important for the control of cell death during mitotic arrest, because it reduces a downstream barrier to apoptosis once caspases-3/7 have been activated after proteolytic destruction of the upstream regulator, Mcl-1 (Harley et al., 2010; Wertz et al., 2011). The time-dependent loss of Mcl-1 releases cytochrome c from mitochondria, resulting in a pro-apoptotic signal that overwhelms the brake set by inhibitory phosphorylation of caspase-9 (Allan and Clarke, 2007), which is also activated by dephosphorylation as mitotic arrest progresses (Harley et al., 2010). The inhibition of XIAP function by phosphorylation would make mitotically-arrested cells less resistant to caspase activitation and may explain the increased sensitivity of such cells to BH3 mimetics that inhibit Mcl-1, Bcl-2 and Bcl-x_L (Colin et al., 2015; Shi et al., 2011). If cells survive mitotic arrest and are released into interphase, dephosphorylation of XIAP would restore its anti-apoptotic function and raise again the threshold for apoptosis.

The sensitisation of mitotically arrested cells to apoptosis can be hypothesised to actively remove cells that become severely delayed in mitosis due to problems with chromosome segregation, supernumerary centrosomes or even aneuploidy. This would provide a mechanism to suppress the propagation of chromosome abnormalities (Figure 8). Cancer cells exhibiting such defects, however, have presumably gone through a selection crisis in which the mechanism of apoptosis during mitosis is actively supressed. Two levels of the pathway at which this might well occur are the over-expression of anti-apoptotic Bcl-2 family proteins, preventing cytochrome c release and caspase activation, or XIAP over-expression, blocking the action of caspases. At present it is unclear if aberrant changes in the post-translational regulation of these components also contribute to the suppression of mitotic cell death in cancer cells, but if this is the case then targeting these mechanisms could activate apoptosis particularly well in such stressed cells.

The regulation of XIAP by CDK1-cyclin B illustrates the close integration of the control of apoptosis with the progression of mitosis. In addition to XIAP, Mcl-1 is destroyed by proteolysis following phosphorylation by CDK1-cyclin B (Harley et al., 2010; Wertz et al., 2011), and the related anti-apoptotic proteins Bcl-2 and Bcl-x_L may be directly inhibited by mitotic phosphorylation (Terrano et al., 2010). Opposing these pro-apoptotic events, we have shown that caspase-9 is inhibited by phosphorylation during normal mitosis and in the early stages of mitotic arrest (Allan and Clarke, 2007). The importance of the inhibition of XIAP by mitotic phosphorylation might be that it removes a downstream brake on apoptosis, resulting in one major point of regulation (caspase-9 activation) that permits the induction of apoptosis after a prolonged arrest. Anti-cancer drugs that target mitotic cells appear to exploit this mechanism to initiate mitosis by arresting or delaying them in mitosis long enough to overcome the temporal restraint to caspase activation. Cells that do not undergo full apoptosis from the mitotic state may nevertheless carry a signal caused by caspase-dependent DNA damage that can subsequently determine long-term cell fate after release into interphase even though a higher threshold for apoptosis has been restored (Colin et al., 2015) (Figure 8). Our results further emphasise that cell death during mitosis is a form of caspase-dependent apoptosis, albeit one under mitosis-specific post-translational controls.

MATERIALS AND METHODS

Cell culture and cell extracts

HeLa (Ohio) and U2OS (HTB96) cell lines were obtained from Cancer Research UK Laboratories, London, UK. HCT116 parental and XIAP knock-out cell lines were purchased from Horizon Discovery Ltd., Cambridge, UK. All cell lines were confirmed as negative for mycoplasma infection. Cells were cultured in DMEM (Invitrogen) supplemented with 10% (v/v) foetal bovine serum (Biosera) and 1% (v/v) Penicillin-Streptomycin (Invitrogen) at 37°C and 5% CO_2. U2OS cells stably expressing GFP-XIAP proteins were generated by transfection with pEGFP-XIAP vector containing a G418 resistance marker. Cells were grown for 2-3 weeks with 800 μg/ml G418 Geneticin (Invitrogen) and maintained in 400 μg/ml G418. Cell extracts were prepared from mitotic or asynchronous HeLa cells at a protein concentration of 6-10 mg/ml in EBS [80 mM β-glycerophosphate-HCl (pH 7.2), 20 mM EGTA-NaOH (pH 8.0), 15 mM $MgCl_2$, 100 mM sucrose, 1 mM DTT, 1 mM PMSF] as described previously (Harley et al., 2010). HeLa cell cytosolic S100 extracts were supplied at a protein concentration of 8 mg/ml in extract buffer [10mM Hepes-KOH (pH 8.5), 10mM KCl, 10mM $MgCl_2$, 0.5mM DTT] (Computer Cell Culture Centre, Mons, Belgium).

XIAP knock down by siRNA

Four RNA oligonucleotides that made up the siGENOME SMARTpool XIAP siRNA (Thermo Fisher Scientific) were tested individually. Two of the four oligonucleotides that resulted in the most efficient depletion of XIAP were used together in future experiments. The two XIAP siRNA oligos and the luciferase control siRNA were:

XIAP siRNA 1: 5'-GCA CGG AUC UUU ACU UUG-3'

XIAP siRNA 2: 5'-GAA CUG GGC AGG UUG UAG A-3'

Luciferase siRNA: 5'-CGU ACG CGG AAU ACU UCG ATT-3'

U2OS cells were transfected with the oligos using Lipofectamine 2000 (Invitrogen) and incubated for 48h. 250 ng/ml nocodazole was then added for a further 48h as required.

Western blotting

Antibodies were used as described in Supplementary Table 1.

Generation of a polyclonal antibody specific for XIAP phosphorylated at Ser40

Rabbits were inoculated with the phosphorylated peptide FANFPSGS*PVSASTL (where S* represents the phosphorylated residue) by Moravian Biotechnology. A phospho-specific antibody, pS40 XIAP, was purified from the serum obtained after a second inoculation on a column of phosphorylated peptide coupled to Reactigel beads (Pierce Biotechnology), eluted with 0.1 M Glycine-HCl (pH 2.5) which was neutralised with the addition of 1.5 M Tris-HCl (pH 8.5) supplemented with 100 μg/ml BSA, 50% glycerol and 0.05% sodium azide, and stored at -20°C.

Phosphorylated or non-phosphorylated peptide was coupled to immunoglobulin-free BSA (Sigma-Aldrich) using 50% (w/v) glutaraldehyde solution (Sigma-Aldrich) diluted in PBS. The BSA-conjugated peptide solutions were serially diluted in PBS, spotted onto nitrocellulose membrane and air-dried before being incubated in Western blocking buffer. They were then incubated with 1:500 diluted phospho-specific antibody overnight at 4°C, followed by washes and secondary antibody probing.

Detection of active caspase-3

Cells on coverslips or glass slides were permeabilised by incubating in ice-cold 80% ethanol for 15 minutes, and followed by two washes in PBS. Cells were blocked in 5% BSA/0.2% Triton-X-100 in PBS for 20 minutes at room temperature, before they were incubated with anti-cleaved caspase-3 antibody (Cell Signalling) at 1:400 dilution in 1% BSA/0.2% Triton-X-100 in PBS at room temperature for 1 h. After two 5-minute washes with 0.2% Triton-X-100/PBS on a rotary shaker, cells were incubated with 1:200 diluted TRITC-anti-rabbit secondary antibody (Dako) and 250 ng/ml DAPI (Sigma) in 1% BSA/0.2% Triton-X-100 in PBS in the dark at room temperature for 1 h. This was followed by two 5 min washes with 0.2% Triton-X-100/PBS and one 5 min wash with PBS on a rotary shaker. Slides were mounted with mounting media (Dako), air dried and kept at 4°C in the dark until viewed under the microscope.

Microscopy

Fixed cells were visualised using Zeiss Axiovert 100 microscope with specific filters for the excitation of fluorophores. Images were taken at 63× magnification using Openlab software. For live-cell imaging, cells were imaged every 10 min in a heated chamber on a Zeiss Axiovert 200M microscope. Images were acquired using a C4742-80-12AG camera

(Hamamatsu) and μmanager software and were processed using ImageJ Fiji. Analysis was carried out on cells that were arrested in mitosis for at least 6 h with cell death being defined by cell morphology and cessation of movement.

Flow cytometry

Cells stained with propidium iodide were analysed on a FACS flow cytometer (Becton Dickinson) on the FL3 channel. A minimum of 10^4 cells were analysed for each sample. Data were displayed as dot plots and histograms showing the cell cycle phases and subG1 population using FlowJo software.

GFP-XIAP precipitation from cells

U2OS cells stably expressing GFP or GFP-XIAP were treated with 100 ng/ml nocodazole for 17 hours. The asynchronous cells from the untreated plate and the mitotically arrested cells from the nocodazole treated plates were washed twice in cold PBS, and lysed in cold GFP lysis buffer [10 mM Tris-HCl (pH 7.5), 150 mM NaCl, 0.5 mM EDTA, 5 mM β-glycerophosphate, 50 mM NaF, 1 mM Na_3VO_4, 1 mM PMSF, 1 μg/ml each of aprotinin, leupeptin and pepstatin A, 0.2% CHAPS]. The protein concentration of the lysates was adjusted to 1 mg/ml with GFP lysis buffer. 300 μg lysate was mixed with 10 μl pre-washed GFP-Trap beads (ChromoTek) for each sample, and incubated at 4°C for 1 h on a rotator. The beads were pelleted by centrifugation at 4°C, washed once with GFP lysis buffer followed by two washes with 10 mM Tris-HCl (pH 7.5). Samples were analysed by SDS-PAGE and Western blotting.

***In vitro* phosphorylation assays**

GST-XIAP was expressed from the pGEX-6P-1 vector in *E.coli* BLR(DE3) competent cells (Novagen), purified on Glutathione Sepharose 4B beads (Amersham) and stored in 10 mM Hepes-KOH (pH 7.5), 150 mM NaCl, 0.07% β-mercaptoethanol. In vitro translated and transcribed (IVT) XIAP was produced using the T_NT Quick Coupled Transcription/Translation system (Promega) using XIAP inserted in the pcDNA3.2/V5-DEST vector. Either 50 ng of GST-XIAP or 3 μl IVT XIAP was incubated with 1 μl mitotic HeLa EBS extract in phosphorylation reaction buffer [50 mM Tris-HCl (pH 7.5), 1 mM DTT] plus MgATP [0.1 mM ATP, 10 mM $MgCl_2$, 5 mM Hepes-KOH (pH 7.5)] at 30°C for 30 min in a total reaction volume of 10 μl. For phosphorylation by CDK1-cyclin B1, 25 ng active

recombinant kinase (Millipore) replaced HeLa extract. Where specified, 1 U/µl calf intestinal phosphatase (CIP) (Roche) and 1 µl of 10× CIP reaction buffer [0.5 M Tris (pH 8.5), 1 mM EDTA], 1 µl of 10× ATP-regenerating system [0.1 mg/ml creatine kinase, 50 mM creatine phosphate], or kinase inhibitors were added. After incubation, reactions were stopped by addition of an equal volume of 2× SDS lysis buffer, 5% β-ME and 0.05% bromophenol blue. Due to the presence of EGTA in the cell extract EBS buffer, which would interfere with PhosTag reagent, an equal molar concentration of $MnCl_2$ was added to the loading samples that were going to be tested on PhosTag gels. Samples were boiled for 4 min, then analysed by SDS-PAGE and Western blotting.

***In vitro* binding assay**

HeLa S100 extract (4mg) was incubated with 10µM cytochrome *c* and 1mM dATP together with ATP regenerating system (1mM ATP, 10µg/ml creatine kinase, 5mM creatine phosphate), 30°C, 3 h. U2OS cells stably expressing GFP-XIAP S40A or S40D were lysed in GFP-Trap buffer [10mM Tris (pH 7.5), 150mM NaCl, 0.5mM EDTA, 0.5% NP40]. 2mg lysate was diluted 2:3 with dilution buffer (GFP-Trap buffer without NP40) and incubated with 25µl GFP-TrapM beads (ChromoTek), 4°C, 1 h with rotation. Beads were isolated using a magnet (BioRad) and washed 3 times in GFP-Trap buffer diluted as above followed by one wash in dilution buffer. GFP-XIAP beads were then incubated with S100/cytochrome *c*/dATP reactions at room temperature, 90 min with rotation. Beads were then isolated, washed as above and boiled in SDS gel-loading buffer.

ACKNOWLEDGEMENTS

Dr Didier Colin provided valuable advice. Phosphorylation site analysis was carried out by the mass spectrometry service in the School of Life Sciences at the University of Dundee. Live-cell imaging was undertaken in the Dundee Imaging Facility.

COMPETING INTERESTS

No competing interests declared.

AUTHOR CONTRIBUTIONS

Y.H. carried out the experiments and analysed the data with the supervision of L.A.A., with the exception of in vitro binding assays and time-lapse microscopy, which were carried out by L.A.A. The study was directed by P.R.C. All authors contributed to preparation of the manuscript.

FUNDING

This work was funded by Cancer Research UK [C275/A13424 to P.R.C.] and a University of Dundee College Studentship [to Y.H].

REFERENCES

Allan, L. A. and Clarke, P. R. (2007). Phosphorylation of caspase-9 by CDK1/cyclin B1 protects mitotic cells against apoptosis. *Mol Cell* **26**, 301-10.

Bekier, M. E., Fischbach, R., Lee, J. and Taylor, W. R. (2009). Length of mitotic arrest induced by microtubule-stabilizing drugs determines cell death after mitotic exit. *Mol Cancer Ther* **8**, 1646-54.

Brito, D. A. and Rieder, C. L. (2006). Mitotic checkpoint slippage in humans occurs via cyclin B destruction in the presence of an active checkpoint. *Curr Biol* **16**, 1194-200.

Budihardjo, I., Oliver, H., Lutter, M., Luo, X. and Wang, X. (1999). Biochemical pathways of caspase activation during apoptosis. *Annu Rev Cell Dev Biol* **15**, 269-90.

Clarke, P. R. and Allan, L. A. (2009). Cell-cycle control in the face of damage--a matter of life or death. *Trends Cell Biol* **19**, 89-98.

Colin, D. J., Hain, K. O., Allan, L. A. and Clarke, P. R. (2015). Cellular responses to a prolonged delay in mitosis are determined by a DNA damage response controlled by Bcl-2 family proteins. *Open Biol* **5**, 140156.

Dan, H. C., Sun, M., Kaneko, S., Feldman, R. I., Nicosia, S. V., Wang, H. G., Tsang, B. K. and Cheng, J. Q. (2004). Akt phosphorylation and stabilization of X-linked inhibitor of apoptosis protein (XIAP). *J Biol Chem* **279**, 5405-12.

Deveraux, Q. L., Leo, E., Stennicke, H. R., Welsh, K., Salvesen, G. S. and Reed, J. C. (1999). Cleavage of human inhibitor of apoptosis protein XIAP results in fragments with distinct specificities for caspases. *EMBO J* **18**, 5242-51.

Du, C., Fang, M., Li, Y., Li, L. and Wang, X. (2000). Smac, a mitochondrial protein that promotes cytochrome c-dependent caspase activation by eliminating IAP inhibition. *Cell* **102**, 33-42.

Durie, D., Lewis, S. M., Liwak, U., Kisilewicz, M., Gorospe, M. and Holcik, M. (2011). RNA-binding protein HuR mediates cytoprotection through stimulation of XIAP translation. *Oncogene* **30**, 1460-9.

Eckelman, B. P., Salvesen, G. S. and Scott, F. L. (2006). Human inhibitor of apoptosis proteins: why XIAP is the black sheep of the family. *EMBO Rep* **7**, 988-94.

Gascoigne, K. E. and Taylor, S. S. (2008). Cancer cells display profound intra- and interline variation following prolonged exposure to antimitotic drugs. *Cancer Cell* **14**, 111-22.

Harley, M. E., Allan, L. A., Sanderson, H. S. and Clarke, P. R. (2010). Phosphorylation of Mcl-1 by CDK1-cyclin B1 initiates its Cdc20-dependent destruction during mitotic arrest. *EMBO J* **29**, 2407-20.

Holcik, M., Yeh, C., Korneluk, R. G. and Chow, T. (2000). Translational upregulation of X-linked inhibitor of apoptosis (XIAP) increases resistance to radiation induced cell death. *Oncogene* **19**, 4174-7.

Huang, H. C., Shi, J., Orth, J. D. and Mitchison, T. J. (2009). Evidence that mitotic exit is a better cancer therapeutic target than spindle assembly. *Cancer Cell* **16**, 347-58.

Kinoshita, E., Kinoshita-Kikuta, E., Takiyama, K. and Koike, T. (2006). Phosphate-binding tag, a new tool to visualize phosphorylated proteins. *Mol Cell Proteomics* **5**, 749-57.

Li, P., Nijhawan, D., Budihardjo, I., Srinivasula, S.M., Ahmad, M., Alnemri, E.S. and Wang, X. (1997). Cytochrome c and dATP-dependent formation of Apaf-1/caspase-9 complex initiates an apoptotic protease cascade. *Cell **91***, 479-489.

Lin, S. C., Huang, Y., Lo, Y. C., Lu, M. and Wu, H. (2007). Crystal structure of the BIR1 domain of XIAP in two crystal forms. *J Mol Biol* **372**, 847-54.

Lu, M., Lin, S. C., Huang, Y., Kang, Y. J., Rich, R., Lo, Y. C., Myszka, D., Han, J. and Wu, H. (2007). XIAP induces NF-kappaB activation via the BIR1/TAB1 interaction and BIR1 dimerization. *Mol Cell* **26**, 689-702.

Mertins, P., Qiao, J. W., Patel, J., Udeshi, N. D., Clauser, K. R., Mani, D. R., Burgess, M. W., Gillette, M. A., Jaffe, J. D. and Carr, S. A. (2013). Integrated proteomic analysis of post-translational modifications by serial enrichment. *Nat Methods* **10**, 634-7.

Nakhaei, P., Sun, Q., Solis, M., Mesplede, T., Bonneil, E., Paz, S., Lin, R. and Hiscott, J. (2012). IkappaB kinase epsilon-dependent phosphorylation and degradation of X-linked inhibitor of apoptosis sensitizes cells to virus-induced apoptosis. *J Virol* **86**, 726-37.

Primorac, I. and Musacchio, A. (2013). Panta rhei: The APC/C at steady state. *J Cell Biol* **201**, 177-89.

Shi, J., Zhou, Y., Huang, H. C. and Mitchison, T. J. (2011). Navitoclax (ABT-263) accelerates apoptosis during drug-induced mitotic arrest by antagonizing Bcl-xL. *Cancer Res* **71**, 4518-26.

Takahashi, R., Deveraux, Q., Tamm, I., Welsh, K., Assa-Munt, N., Salvesen, G. S. and Reed, J. C. (1998). A single BIR domain of XIAP sufficient for inhibiting caspases. *J Biol Chem* **273**, 7787-90.

Tamm, I., Kornblau, S. M., Segall, H., Krajewski, S., Welsh, K., Kitada, S., Scudiero, D. A., Tudor, G., Qui, Y. H., Monks, A. et al. (2000). Expression and prognostic significance of IAP-family genes in human cancers and myeloid leukemias. *Clin Cancer Res* **6**, 1796-803.

Terrano, D. T., Upreti, M. and Chambers, T. C. (2010). Cyclin-dependent kinase 1-mediated Bcl-xL/Bcl-2 phosphorylation acts as a functional link coupling mitotic arrest and apoptosis. *Mol Cell Biol* **30**, 640-56.

Uetake, Y. and Sluder, G. (2010). Prolonged prometaphase blocks daughter cell proliferation despite normal completion of mitosis. *Curr Biol* **20**, 1666-71.

Vassilev, L. T., Tovar, C., Chen, S., Knezevic, D., Zhao, X., Sun, H., Heimbrook, D. C. and Chen, L. (2006). Selective small-molecule inhibitor reveals critical mitotic functions of human CDK1. *Proc Natl Acad Sci USA* **103**, 10660-5.

Verhagen, A.M., Ekert, P.G., Pakusch, M., Silke, J., Connolly, L.M., Reid, G.E., Moritz, R.L., Simpson, R.J. and Vaux, D.L. (2000). Identification of DIABLO, a mammalian protein that promotes apoptosis by binding to and antagonizing IAP proteins. *Cell* **102,** 43-53.

Wertz, I. E., Kusam, S., Lam, C., Okamoto, T., Sandoval, W., Anderson, D. J., Helgason, E., Ernst, J. A., Eby, M., Liu, J. et al. (2011). Sensitivity to antitubulin chemotherapeutics is regulated by MCL1 and FBW7. *Nature* **471**, 110-4.

Figures

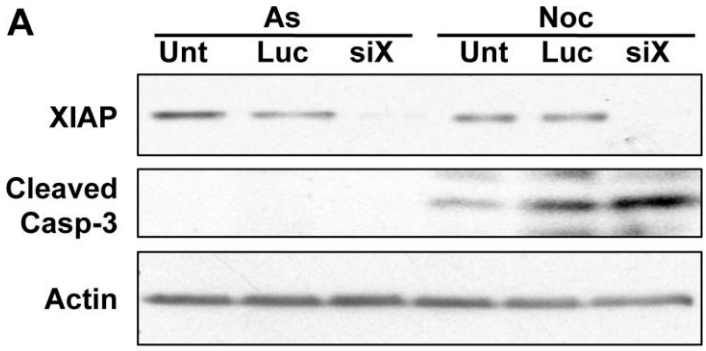

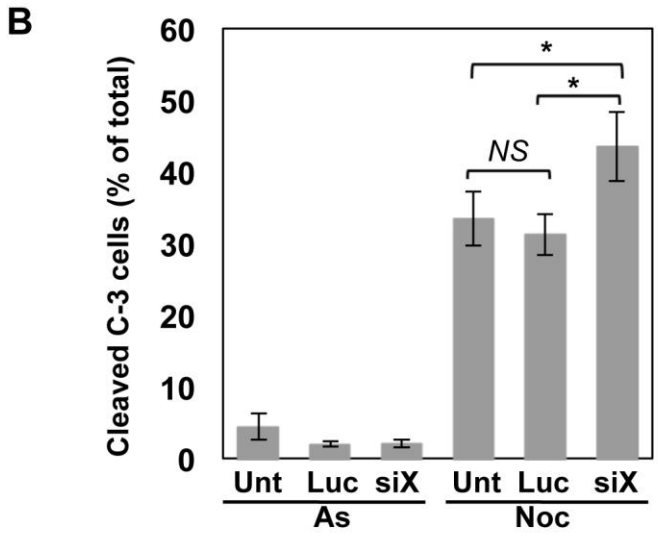

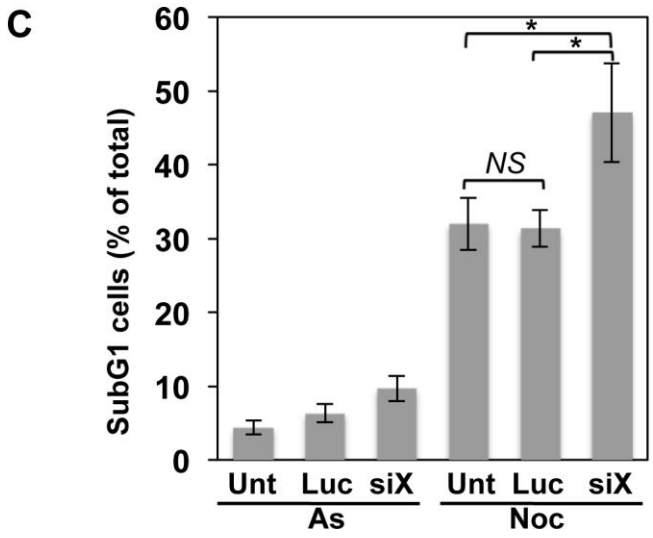

Figure 1. Endogenous XIAP restrains apoptosis in response to mitotic arrest.

Knock down of endogenous XIAP results in increased caspase-3 activity and apoptois in response to prolonged mitotic arrest. U2OS cells were either untrasfected (Unt), transfected with siRNA directed against luciferase as control (Luc) or XIAP (siX) for 48 h and then either untreated (asynchronous, As) or treated with 250 ng/ml nocodazole for a further 48 h (Noc).

(A,B) Generation of active, cleaved caspase-3 was analysed by (**A**) SDS-PAGE and Western blotting, or (**B**) fluorescence microscopy. In (B), at least 300 cells were counted for each category in every experiment (n=4). Error bars represent ±SD, *NS* = non-significant difference, *statistically significant difference, $P<0.05$.

(**C**) Apoptosis was analysed by subG1 DNA content by flow cytometry (n=3). Error bars represent ±SD, *NS* = non-significant difference, *statistically significant difference, $P<0.05$.

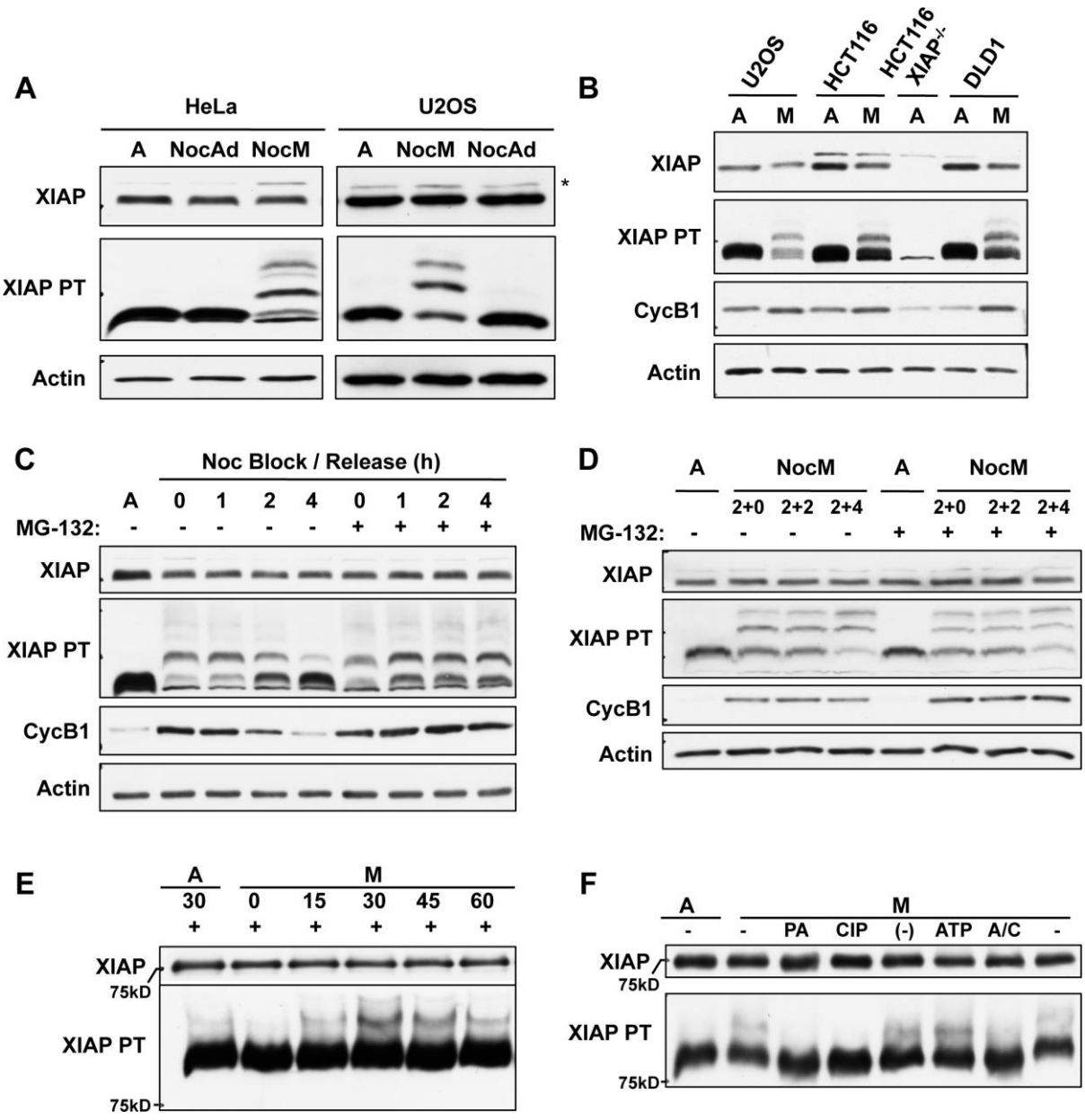

Figure 2. XIAP is phosphorylated in mitotically arrested cells.

(**A**) **Analysis of XIAP phosphorylation on PhosTag gels.** HeLa and U2OS cells were treated with 100 ng/ml nocodazole for 17 h and harvested as either non-adherent nocodazole mitotic (NM) or nocodazole adherent interphase (NAd) samples. Untreated asynchronous cells (A) were used as a control. Samples were analysed on SDS-PAGE with or without the addition of PhosTag (PT) as indicated. * denotes a non-specific band detected by XIAP antibody.

(B) XIAP is phosphorylated in mitotically arrested cells. U2OS, HCT116 and DLD-1 cells were treated with 100 ng/ml nocodazole for 17 h. The non-adherent nocodazole mitotic (M) samples were collected, and samples were analysed by SDS-PAGE and Western blotting.

(C) XIAP phosphorylation is mitosis-specific and the protein is dephosphorylated as cells exit mitosis. U2OS cells were either untreated (A) or treated with 100 ng/ml nocodazole for 17 h before the rounded up cells were either lysed, or replated in nocodazole-free media in the absence or presence of 10 μM of the proteasome inhibitor, MG132, for a further 1, 2, or 4 h. Samples were analysed by SDS-PAGE with or without the addition of PhosTag as indicated, and Western blotting using the indicated antibodies.

(**D**) **XIAP is continuously phosphorylated during mitosis and the phosphorylated form is stable.** U2OS cells were either untreated (A) or pre-treated with 10 μM MG132 for 2 h, before adding 100 ng/ml nocodazole to the media and leaving for 2 h. The rounded up mitotic cells were then isolated, and either lysed or replated in the same media for a further 2 or 4 h. The floating cells were collected at the end of the time course. Samples were analysed by SDS-PAGE, and immunoblotted with indicated antibodies.

(E) Recombinant GST-XIAP is phosphorylated in mitotic cell extract. Asynchronous (A) and nocodazole-treated mitotic (M) HeLa cell extracts were incubated with recombinant GST-tagged XIAP protein for the indicated time. Reactions were terminated by the addition of 2× SDS lysis buffer and samples were analysed by SDS-PAGE and Western blotting.

(F) Phosphorylation of GST-XIAP is inhibited by a CDK inhibitor or phosphatase. *In vitro* phosphorylation reaction in mitotic (M) cell extracts was carried out for 30 min in the presence of 10 μM purvalanol A (PA), 0.4 U calf intestinal phosphatase (CIP), phosphatase buffer (–), ATP-regenerating system (ATP) or both ATP-regenerating system and CIP (A/C). Samples were analysed by SDS-PAGE and Western blotting. A lysate prepared from untreated asynchronous cells (A) was used as a control.

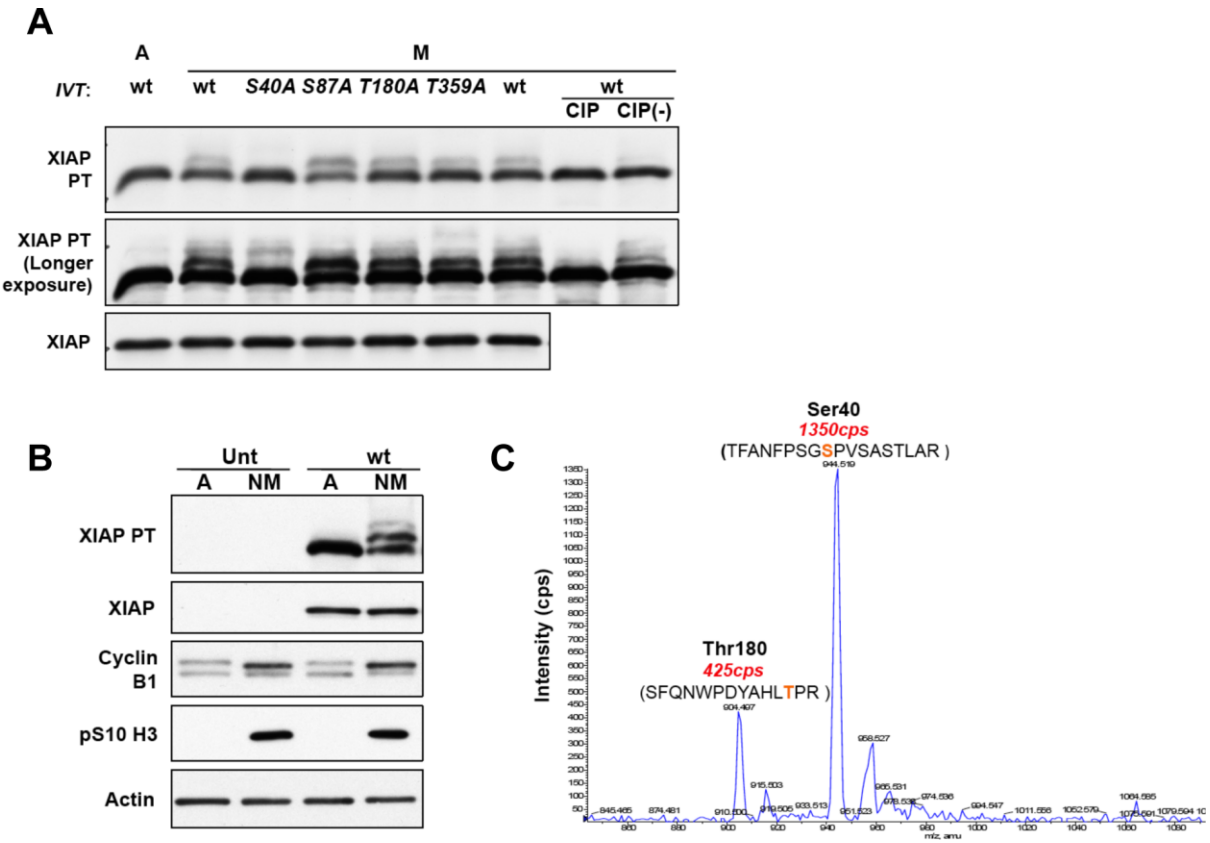

Figure 3. Identification of sites in XIAP phosphorylated in mitosis.

(**A**) **In vitro translated (IVT) XIAP is phosphorylated in mitotic cell extract.** Wild-type (wt) and four mutant XIAP proteins were expressed *in vitro* to a similar level by IVT and added to extracts from asynchronous (A) or mitotically-arrested HeLa cells to a level much greater than endogenous XIAP protein. Nocodazole-treated mitotic extract (M) was also incubated with wild-type protein in the presence of calf intestinal phosphatase (CIP) or phosphatase storage buffer (CIP(-)) to confirm the phosphorylation. Reactions were terminated by the addition of 2× SDS lysis buffer, and the samples were analysed by SDS-PAGE and Western blotting.

(B,C) GFP-tagged XIAP is mitotically phosphorylated at Ser40. (B) U2OS cells that were either untransfected (Unt) or stably expressing GFP-tagged wild-type XIAP (wt) were treated with 100 ng/ml nocodazole for 17 h. The floating mitotic cells were collected at the end of the treatment and analysed by PhosTag SDS-PAGE and western blotting. **(C)** GFP-XIAP was precipitated from 2.2 mg cell lysate of mitotically arrested U2OS XIAP wild-type cells that had been treated with 100 ng/ml nocodazole for 24 h. GFP-XIAP was immunoprecipitated using GFP-Trap beads and analysed by mass spectrometry of tryptic peptides.

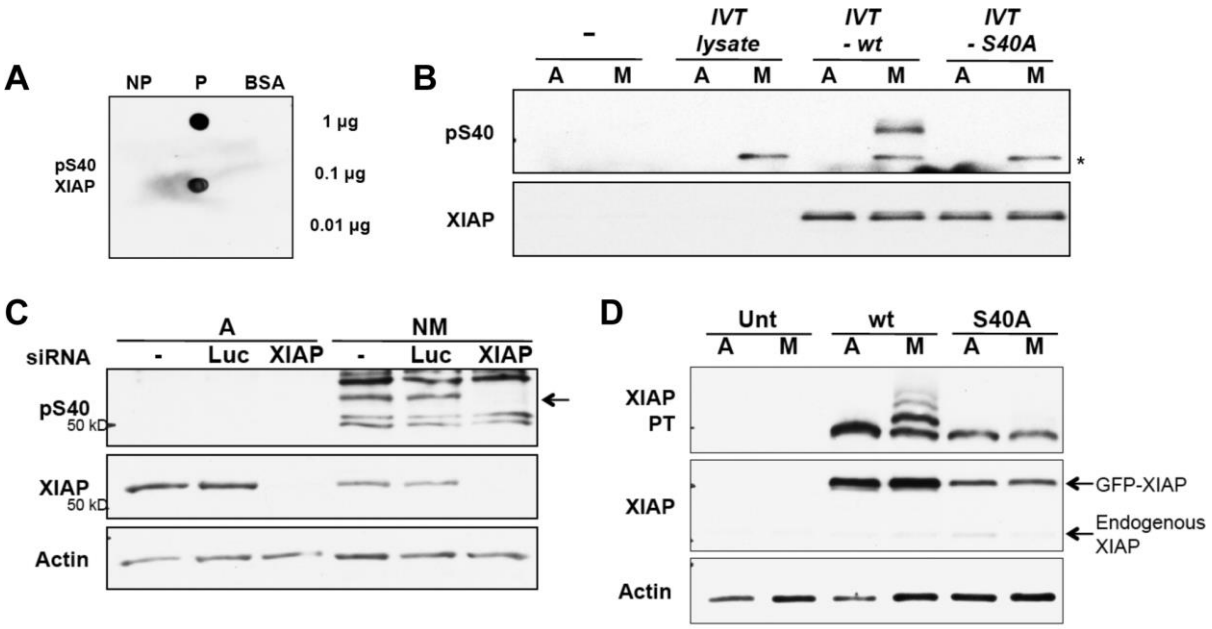

Figure 4. XIAP is phosphorylated at Ser40 in mitotic cells.

(A) An antibody generated against pS40 XIAP is specific for the phosphopeptide. Decreasing amounts of the non-phospho-peptide (NP), phospho-peptide (P) and BSA control were spotted onto nitrocellulose membranes. The membranes were immunoblotted with 1:500 diluted phospho-antibody purified from serum.

(B) The pS40 antibody specifically recognizes XIAP phosphorylated at Ser40. Wild-type (wt) and S40A mutant XIAP protein were generated using IVT, and the reaction mix for each protein was incubated with either asynchronous (A) or mitotic arrested (M) HeLa cell extract. Samples were analysed by SDS-PAGE and Western blotting. The IVT reaction mix incubated without vector DNA was used as an extra negative control (IVT lysate), which showed that the non-specific band (*) was a protein present in the reticulocyte lysate that was phosphorylated by HeLa mitotic extract.

(C) Endogenous XIAP is phosphorylated at Ser40 in cells. U2OS cells were transfected with siRNA against XIAP or Luciferase (Luc). 48 h post-transfection, cells were either untreated (A) or treated with 250 ng/ml nocodazole for 24 h (NM). All cells were collected from untreated samples and the floating cells were collected from nocodazole-treated samples. Cells were lysed, analysed by SDS-PAGE and immunoblotted with pS40 antibody. Phosphorylated XIAP, which is ablated by the specific siRNA, is indicated by an arrow.

(D-F) Ser40 is required for XIAP phosphorylation in cells. U2OS cells which were untransfected (Unt) or stably expressing GFP-XIAP wild-type (wt) or S40A were either untreated (A) or treated with 100 ng/ml nocodazole for 17 h. The floating cells were collected from nocodazole treated samples. All cell lysates were analysed by SDS-PAGE and immunoblotted with indicated antibodies. In (**D**), samples were analysed on a PhosTag (PT) gel. In (**E**), adherent interphase cells (NAd) from nocodazole treated samples were also analysed. In (**F**), cell lysates were incubated with GFP-Trap beads and GFP-tagged proteins were immunoprecipitated from the samples. Lysates which were not incubated with beads were used as input samples.

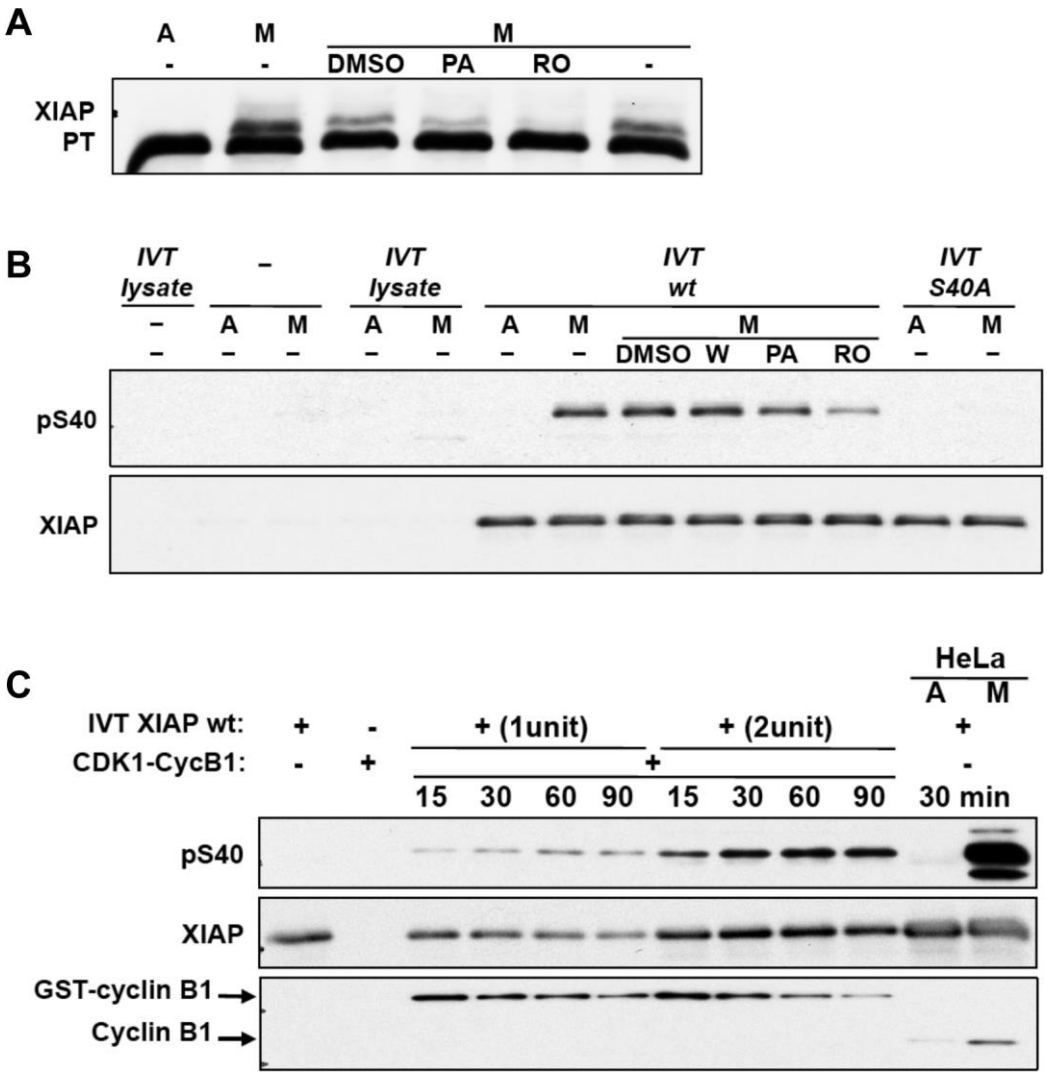

Figure 5. XIAP is phosphorylated at Ser40 by CDK1-cyclin B.

(A) CDK1 kinase inhibitors suppress phosphorylation of XIAP *in vitro*. Wild-type XIAP produced by coupled in vitro translation/transcription (IVT XIAP) was incubated with asynchronous (A) or mitotic nocodazole-treated (M) HeLa cell extracts with or without kinase inhibitors purvalanol A (PA, 10 μM) and RO 3306 (RO, 10 μM). Lysates were analysed by PhosTag (PT) SDS-PAGE and immunoblotted with XIAP antibody.

(B) Wild-type (wt) IVT XIAP was incubated with asynchronous (A) or mitotic nocodazole-treated (M) HeLa cell extracts at 30°C for 30 min with or without kinase inhibitors. Wortmannin (W) was used at 0.1 μM. PA and RO as in (A). IVT reticulocyte lysate without vector DNA, HeLa extracts incubated alone, IVT lysate without vector DNA incubated with HeLa extracts and IVT S40A mutant incubated with HeLa extracts were used as negative controls. Reactions were analysed by SDS-PAGE and immunoblotted with pS40 XIAP antibody.

(**C**) **Ser40 of XIAP is phosphorylated by CDK1-cyclin B1.** Active recombinant GST-tagged CDK1-cyclin B1 was incubated with two different amounts of wild-type IVT-XIAP at 30°C over varying times as indicated. IVT XIAP alone, CDK1-cyclin B1 alone, and IVT XIAP incubated with HeLa extracts were used as controls. Reactions were stopped by the addition of 2× SDS lysis buffer. Samples were analysed by SDS-PAGE and Western blotting.

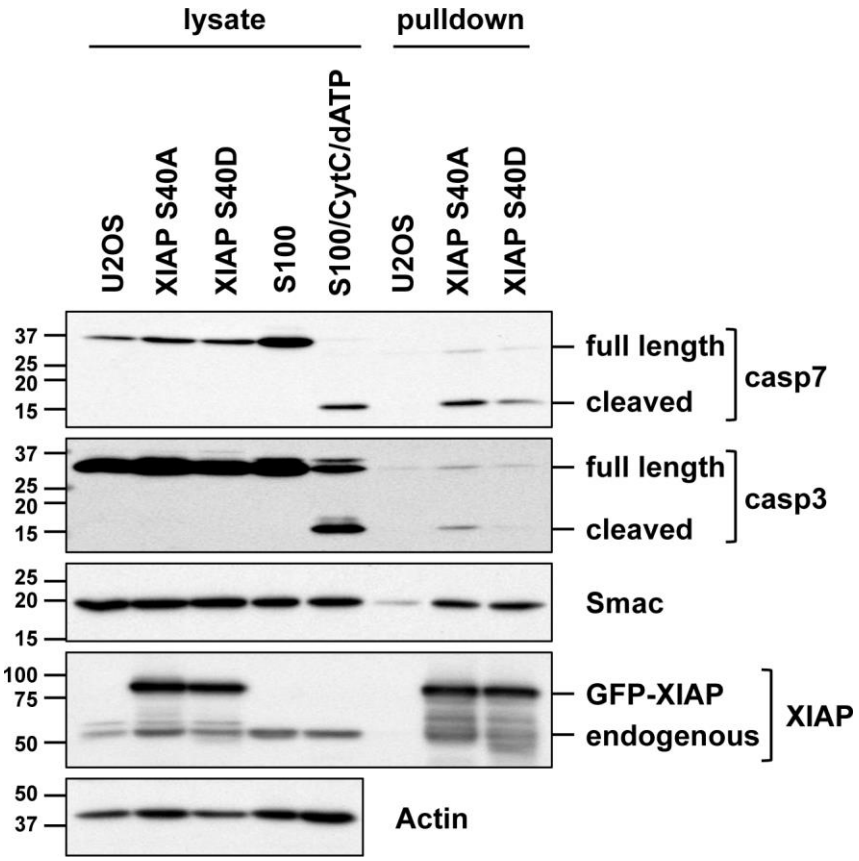

Figure 6. The ability of XIAP to bind cleaved effector caspases is inhibited by mutation of Ser 40 to phosphomimetic aspartate.

HeLa S100 extract was incubated with cytochrome c and dATP to induce caspase cleavage prior to incubation with GFP-XIAP precipitated from cells stably expressing GFP-XIAP S40A or S40D protein. GFP-XIAP was recovered from the extract and co-precipitating proteins were detected by western blotting using the indicated antibodies. Cell lysates and HeLa cell S100 reactions were analysed for comparison.

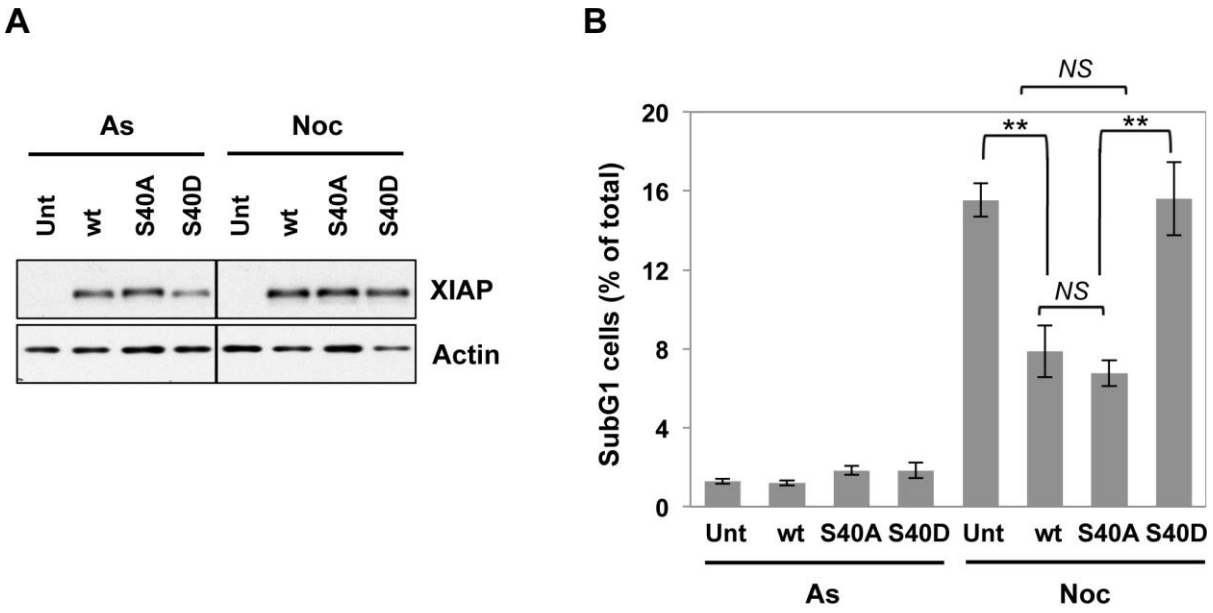

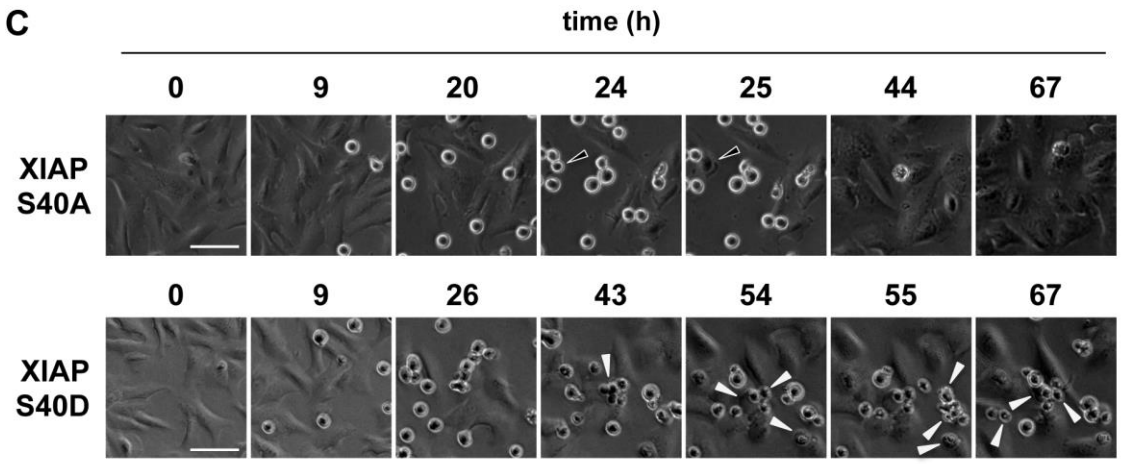

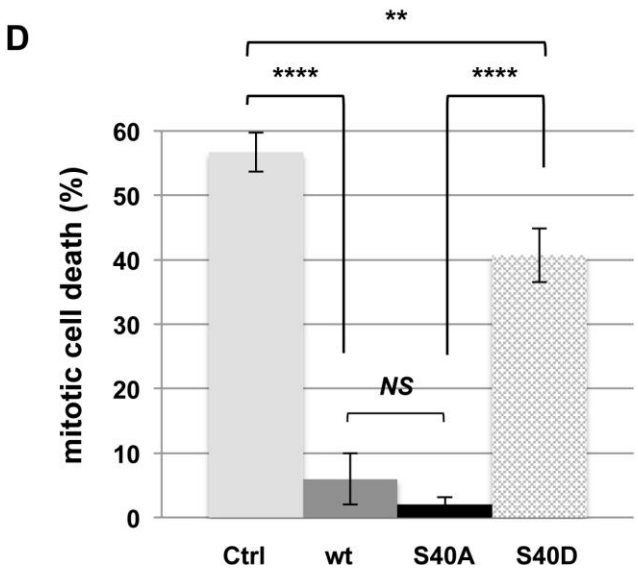

Figure 7. Mutation of Ser40 in XIAP to phosphomimetic aspartate inhibits its ability to protect cells against apoptosis induced by prolonged mitotic arrest.

(A,B) Cell death following mitotic arrest is not inhibited by expression of XIAP S40D protein. U2OS cells which were untransfected (Unt), stably expressing GFP-tagged wild-type (wt), S40A or S40D mutant XIAP protein were treated with 250 ng/ml nocodazole for 48 h. All cells were collected at the end of the time course and either **(A)** lysed, analysed by SDS-PAGE and Western blotting (representative blots are shown) or **(B)** fixed and stained with PI for sub G1 analysis using flow cytometry (n=3). In (B), error bars represent ±SD, *NS* = non-significant difference. Significant difference, ***P*<0.005.

(C,D) XIAP S40D fails to restrain apoptosis during mitotic arrest. Cells stably expressing GFP-tagged wild-type (wt), S40A or S40D mutant XIAP protein were treated with 250 ng/ml nocodazole. Cell fate following mitotic entry was monitored by time-lapse microscopy. **(C)** Representative images of cells expressing S40A or S40D mutant XIAP are shown. Examples of cells undergoing slippage (open arrows) or mitotic cell death (full arrows) are indicated. Scale bar = 50µm. **(D)** Quantification of mitotic cell death in cell lines depicted in (C), control cells (Ctrl) and cells expressing wild-type XIAP (wt). For each experiment (n=3), the fate of 50 cells was assessed. Error bars represent ±SD. *NS* = non-significant difference. Significant differences ***P*<0.01, *****P*<0.0001.

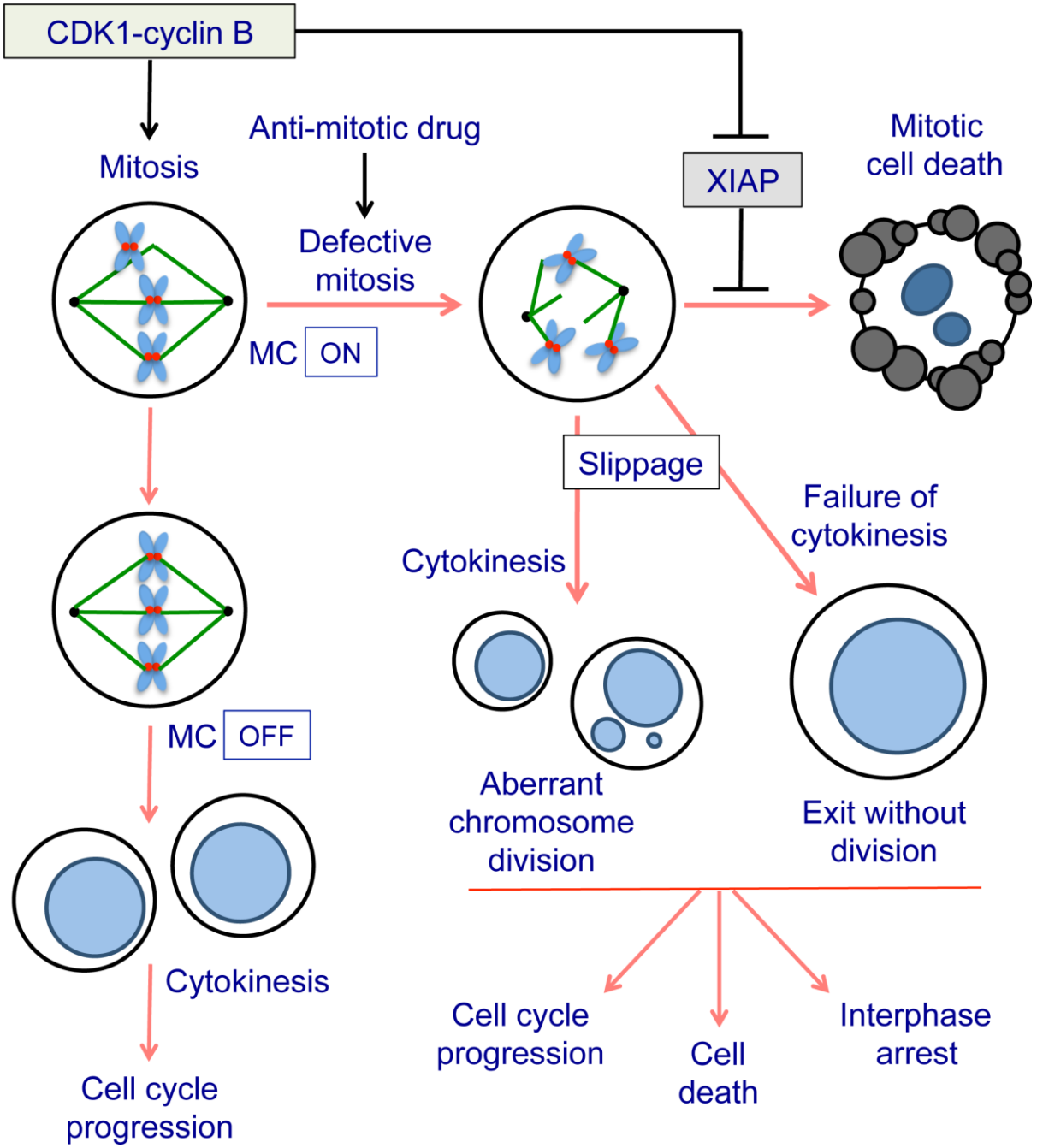

Figure 8. Role of XIAP in determining cell fate during mitotic arrest.

CDK1-cyclin B1 drives cells into mitosis and controls the induction of apoptosis by inhibitory phosphorylation of XIAP. After the last unattached kinetochore is correctly attached to spindle microtubules and the chromosomes are properly aligned, the spindle assembly or mitotic checkpoint (MC) is switched off. CDK1 is then inactivated as cyclin B is rapidly degraded, and cells progress through anaphase, undergo cytokinesis and exit mitosis. In the presence of an anti-mitotic drug such as a microtubule poison, the checkpoint cannot be satisfied and cells are arrested for a prolonged period. Arrested cells may undergo cell

death or can slip out of mitosis due to the slow degradation of cyclin B and undergo a variety of alternative cell fates. Phosphorylation of XIAP reduces the threshold for apoptosis during mitotic arrest. However, when a cell exits mitosis normally or slips out of mitotic arrest, XIAP is reactivated by dephosphorylation and contributes to cell survival.

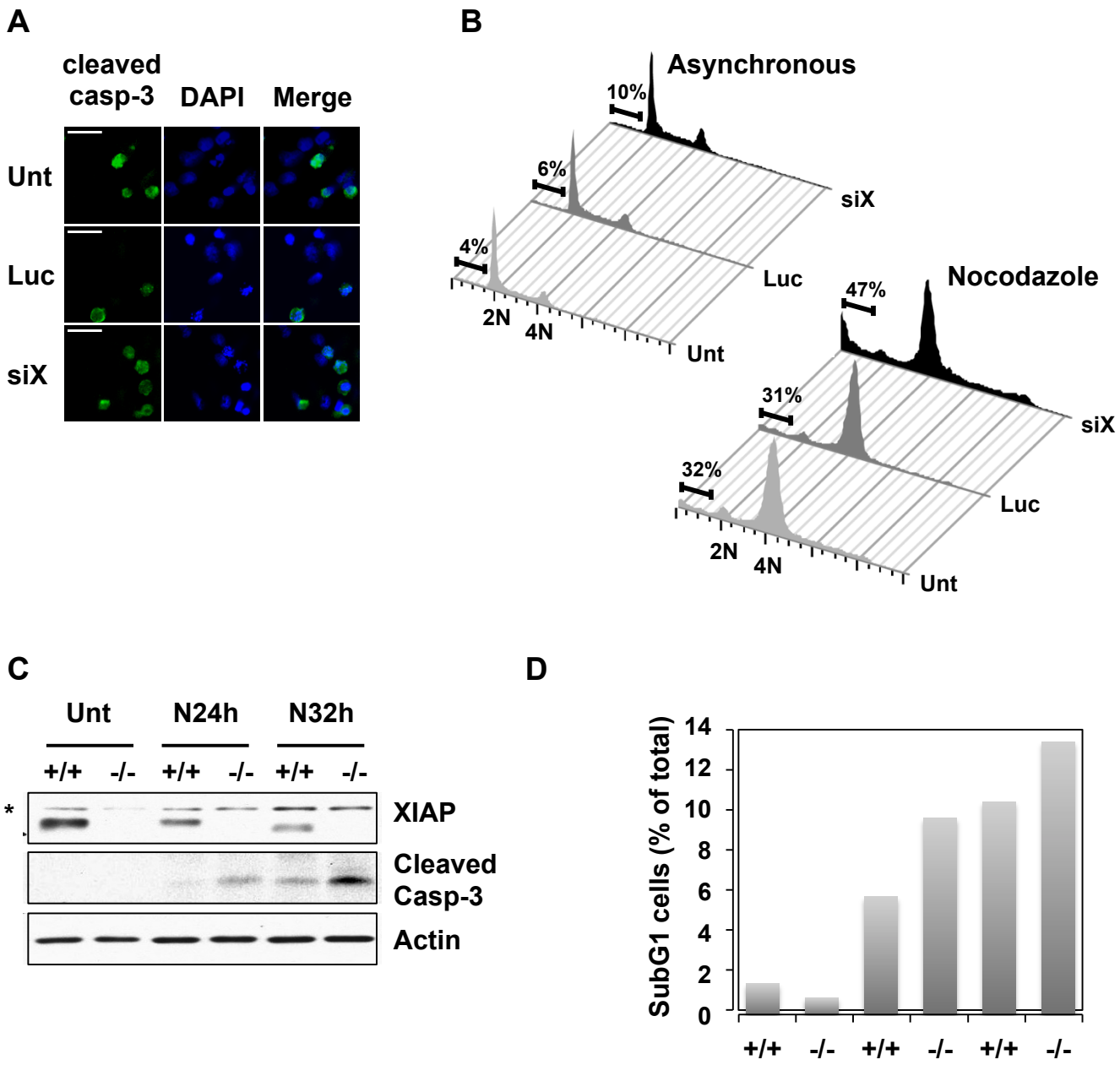

Figure S1. XIAP restrains apoptosis in response to prolonged mitotic arrest.
(A,B) U2OS cells were untransfected (Unt) or transfected with siRNA against luciferase (Luc) or XIAP (siX) for 48 h and then treated with 250ng/ml nocodazole for a further 48 h. **(A)** Representative images of cleaved caspase-3 immunofluorescence. DNA was visualised with DAPI. Scale bar = 50µm. **(B)** Cell cycle profile from the flow cytometry analysis of subG1 population in asynchronous and nocodazole treated cells. The graphs were generated using the software FlowJo. Cells were stained with PI and sorted according to their DNA content (propidium iodide staining) along the X-axis. Cells with less than 2N DNA content (subG1) were considered apoptotic.
(C,D). Human HCT116 cells which were either wild type (+/+) or XIAP null (-/-), were untreated (Unt) or treated with 250 ng/ml nocodozole for 24 (N24h) or 32 h (N32h), after which time all the cells on the plate were harvested and analysed. (**C**) Cells were lysed and analysed by SDS-PAGE and immunoblotting with antibodies to XIAP, cleaved (active) caspase-3 and actin as a loading control. * Indicates a non-specific band detected by the XIAP antibody. (**D**) Cells were fixed and stained with propidium iodide for analysis of subG1 DNA content using flow cytometry.

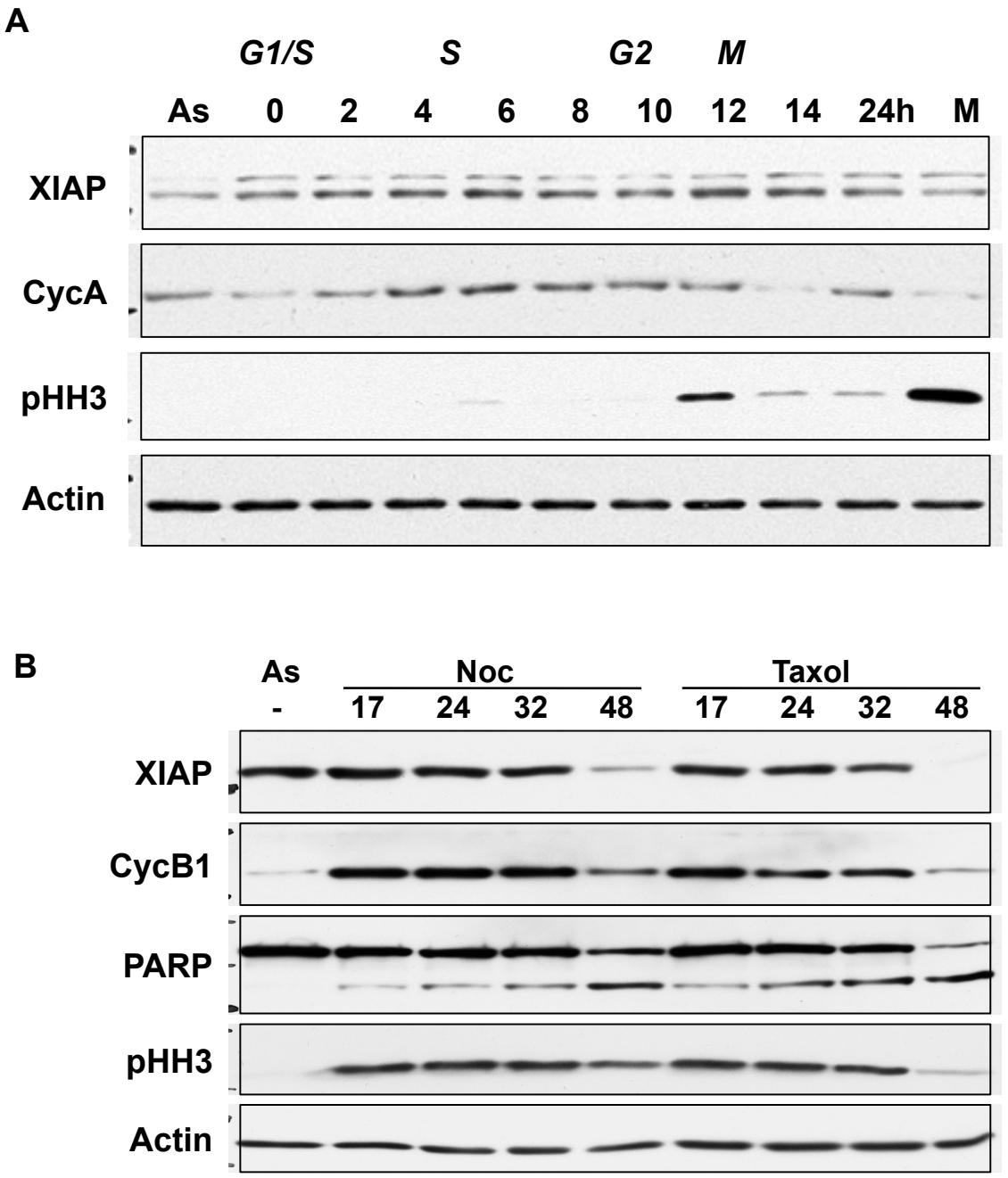

Figure S2. Level of XIAP does not vary periodically during the cell cycle.
(**A**) U2OS cells were synchronised at the G1/S boundary by double thymidine block, released into fresh media and harvested at the times indicated (0-24h). The approximate timing of S, G1 and M phases are indicated. Samples were blotted with antibodies as indicated. Cell lysates from asynchronous (As) and untreated mitotic (M) cells were used as controls.
(**B**) U2OS cells were treated with 100 ng/ml nocodazole (Noc) or 100 nM paclitaxel (Taxol) for 17-48 h and rounded up mitotic and apoptotic cells were collected. A cell lysate from asynchronous cells (As) was used as a control. Samples were blotted with antibodies as indicated. Loss of XIAP coincides with exit from mitosis, indicated by loss of cyclin B1 and phospho-Ser10 Histone H3, and the onset of apoptosis, indicated by the cleavage of PARP to generate a faster migrating form.

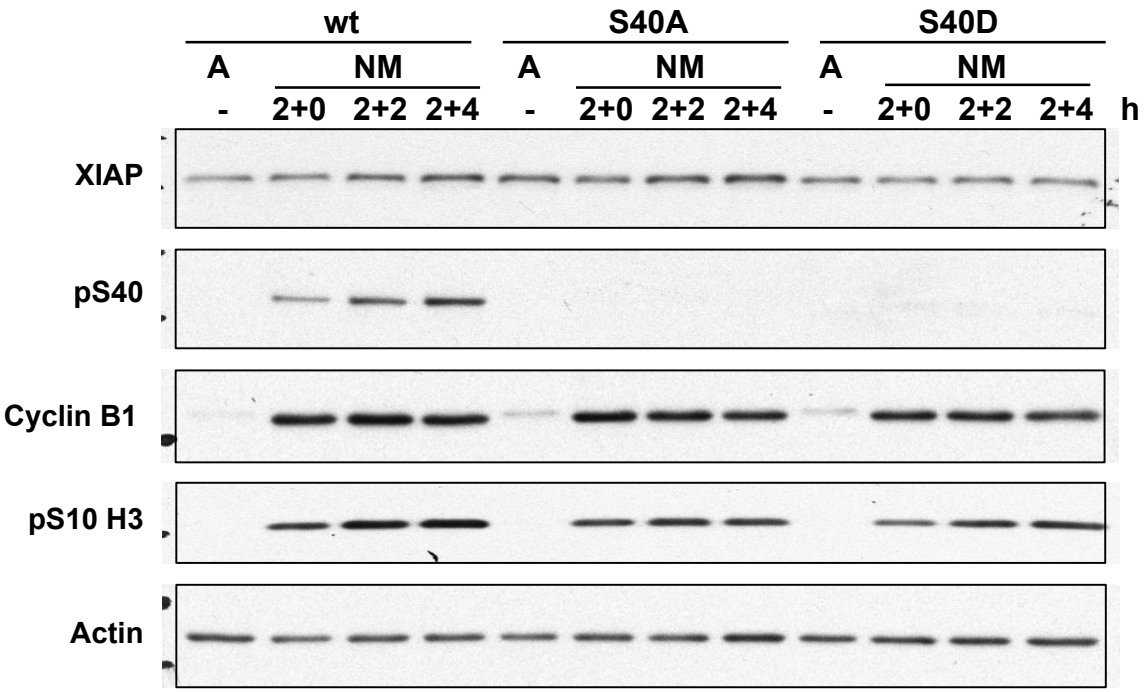

Figure S3. S40A and S40D mutant XIAP proteins remain stable during a short mitotic arrest. Cells stably expressing GFP-tagged wild-type (wt), S40A or S40D XIAP were treated with 100 ng/ml nocodazole for 2 h, before the floating population was isolated and replated in the same nocodazole-containing media for another 2 or 4 h. The nocodazole-treated cells (NM) were analysed alongside untreated asynchronous cells (A) by SDS-PAGE, and immunoblotted with XIAP phospho-specific antibody pS40 and mitotic markers Cyclin B1 and pS10 H3.

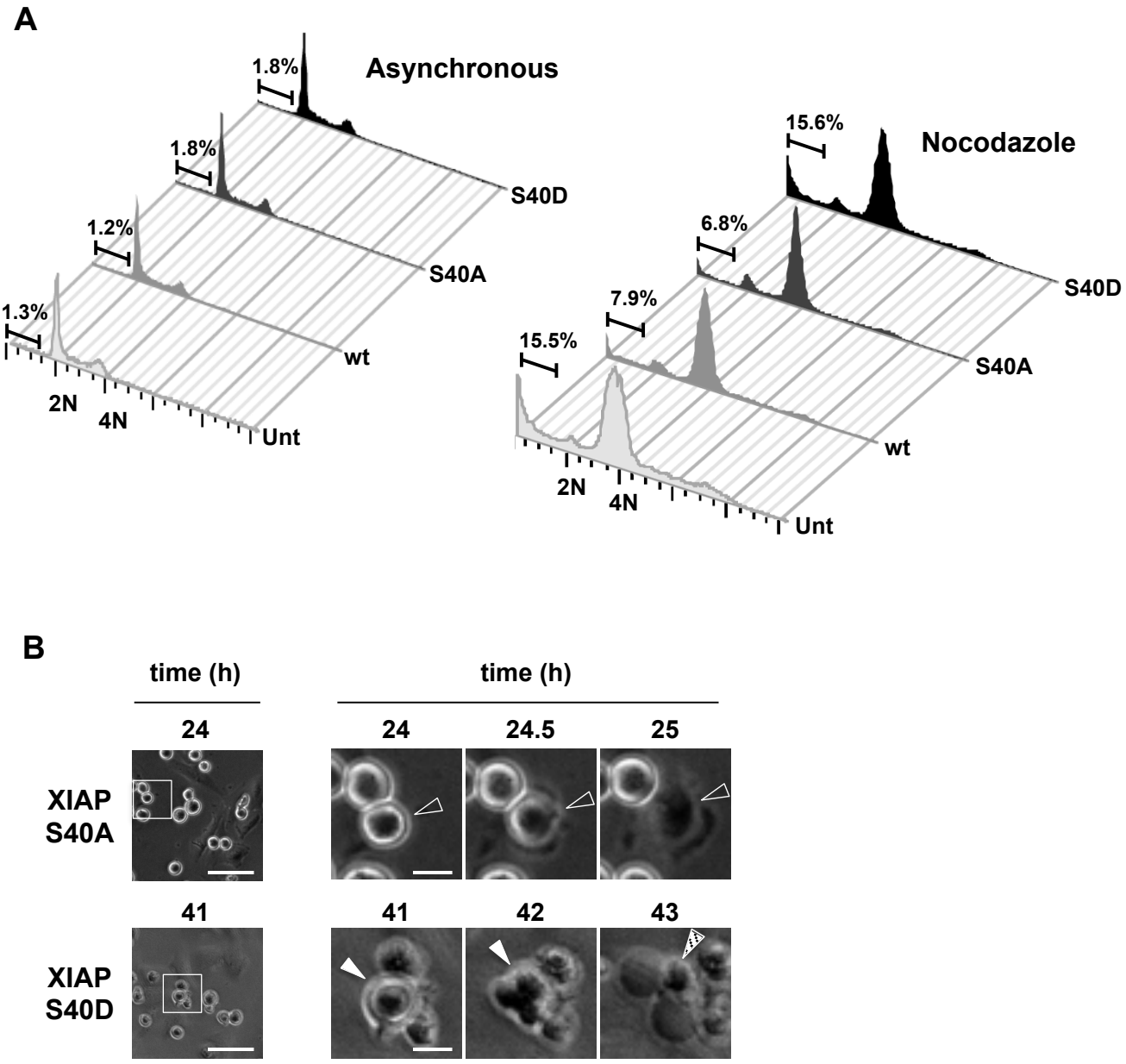

Figure S4. Over-expression of S40D XIAP does not protect cells from cell death in a prolonged mitotic arrest.

(A) The cell cycle profile from the flow cytometry analysis of cell death in untransfected or stable cell lines that were either untreated (asynchronous) or treated with nocodazole. The graphs were generated using the software FlowJo. Cells were stained with PI and sorted according to their DNA content along the X-axis. Cells with less than 2N DNA content (SubG1) were considered apoptotic.

(B) U2OS cells stably expressing GFP-tagged S40A or S40D mutant XIAP protein were treated with 250ng/ml nocodazole. Cell fate following mitotic entry was followed by time lapse microscopy. Right hand panels show enlarged images of cells indicated (boxed) in left hand panels at 24-25 h (S40A) or 41-43 h (S40D). Examples of cells undergoing mitotic slippage (open arrow) or mitotic cell death (full arrow) are shown. The hatched arrow indicates the residual cell body following mitotic cell death. Scale bar = 50µm (left hand panels), 10µm (right hand panels).

Phosphorylation of XIAP by CDK1-cyclin B controls mitotic cell death

Ying Hou, Lindsey A. Allan and Paul R. Clarke

Supplementary Table 1. Antibodies

Primary antibodies

Primary antibody	Molecular weight (kDa)	Species	Dilutions for WB/IF	Supplier (cat. No.)
Actin	42	Rabbit	1:5000	Sigma (#A2066)
Caspase-3	32	Mouse	1:1000	BD Biosciences (#610322)
Cleaved caspase-3	17	Rabbit	1:1000	Cell Signalling (#9661)
Cleaved caspase-3	17	Rabbit	IF 1:400	Cell Signalling (#9661)
Caspase-9	47	Mouse	1:1000	Chemicon (MAB4609)
Cyclin A	60	Mouse	1:1000	BD Biosciences (#611269)
Cyclin B1	55	Rabbit	1:1000	Santa Cruz (#sc-752)
GFP	27	Rabbit	1:1000	Santa Cruz (#sc-8334)
GST	26	Rabbit	1:10000	Santa Cruz (#sc-459)
pS10 HH3	17	Rabbit	1:2500	Millipore (#09-797)
PARP	116	Mouse	1:1000	AbD Serotec (MCA1522G)
XIAP	57	Mouse	1:10000	BD Biosciences (#610762)
pS40 XIAP	57	Rabbit	1:250	Described in this publication

Secondary antibodies

Secondary antibody	Species raised in	Dilutions for WB/IF	Supplier (cat. No.)
Anti-mouse-HRP	Goat	1:5000	Bio-Rad (#170-6516)
Anti-rabbit-HRP	Goat	1:5000	Bio-Rad (#170-6515)
Anti-rabbit-TRITC	Swine	IF 1:200	Dako (#R0156)